J Therm Anal Calorim (2015) 119:1963–1970
DOI 10.1007/s10973-014-4353-7

AgNPs polypropylene gel films–thermal study and antibacterial activity

Washington Luiz Oliani · Luis Filipe Carvalho Pedroso de Lima · Sizue Ota Rogero · Humberto Gracher Riella · Ademar Benevolo Lugao · Duclerc Fernandes Parra

Received: 15 August 2014 / Accepted: 13 December 2014 / Published online: 31 January 2015

Abstract In this work, antibacterial activity was investigated in polypropylene gel containing silver nanoparticles (AgNPs). The PP was modified by crosslink under gamma radiation process of pristine PP, in acetylene atmosphere and dose of 12.5 kGy, followed by thermal treatment. The thin films of the polypropylene gel (AgNPs-GelPP) were obtained by extraction in boiling xylene for period of 12 h at 138 °C, followed by decantation at room temperature of 25 °C. The films of AgNPs-GelPP were characterized using scanning electron microscopy, energy-dispersive spectroscopy, transmission electron microscopy (TEM), differential scanning calorimetry (DSC), and X-ray diffraction. Cytotoxicity tests and reduction of the colony forming number unit were performed in the films. Efficiency of the silver nanoparticles on antibacterial activity was evaluated and analyzed versus DSC. The results showed that crystallinity cooperates to bactericidal effect.

Keywords Microgel · Modified PP · Silver nanoparticles · Crosslinking · Antibacterial activity

Introduction

Developments of branched polypropylene (iPP) have been reported considering the grafting of long chain branches on PP backbone when using acetylene as a crosslinker, under gamma radiation process. The grafting reactions occur by rearrangement of the radicals formed by radiation in the polymer [1, 2].

When polyolefins are subject to ionizing radiation, two main effects occur: crosslink and scission of macromolecules [3, 4]. Alternatively it can be postulated that in the branching of polymer both crosslinking and main chain degradation occur simultaneously and the chain scission process requires a higher overall activation energy than crosslinking [4].

In recent work with polypropylene nonwovens exposed to dose up to 25 kGy was reported the effect of γ-irradiation on the degradation of spunbond and meltblown polypropylene in great detail [5]. The degradation process of polypropylene exposed to gamma radiation dose from 5 to 100 kGy under inert atmosphere reveals mechanisms of chain scission and chain branching [6]. In the radiation process the loose ends of broken chains created, in the aftermath of multi-ionization spurs, in polypropylene results in the reduction of average molecular weight, while in polyethylene can form crosslinked structures with neighboring chains. The radiation yield of chain scission in polymers is treated as a measure of the radiation yield of multi-ionization spurs [7]. Polymers absorb the energy of ionizing radiation in a heterogeneous form [8] and in amorphous region there is a variety of sizes of spurs [9] that form nucleation points where microgels and nanogels appear [10, 11].

The literature reports for isotactic polypropylene (iPP) gels, obtained from toluene and o-xylene solutions, the melting temperature dependency on polymer concentration, as on molecular weight. It increases gradually with increase of both. The results showed somewhat different network structures of the gels with spherulites in contact

W. L. Oliani (✉) · L. F. C. P. de Lima · S. O. Rogero · A. B. Lugao · D. F. Parra
Nuclear and Energy Research Institute, IPEN-CNEN/SP, Av. Prof. Lineu Prestes, 2242–Cidade Universitária, São Paulo, SP 05508-000, Brazil
e-mail: washoliani@usp.br

H. G. Riella
Federal University of Santa Catarina, UFSC-University Campus-CEP, Florianópolis, SC 88040-900, Brazil

with each other and bonded with crystalline ties. This evidence indicates that those spherulites and crystalline ties form a three-dimensional network structure [12].

Parallel to the investigation of how those micro and nanogels are formed, it has been speculate if nano-dispersion silver particles are observed in films of AgNPs-GelPP. In base of this hypothesis, it would be opportune to investigate the antimicrobial activity of AgNPs inserted in PP modified by radiation process [13].

Since ancient times, silver has been most extensively studied among various antimicrobial agents and used against infections or to prevent spoilage. At present, many researchers have focused on antibacterial and multi-functional properties of silver nanoparticles [13].

Silver in its metallic state can react with moisture releasing highly reactive Ag^{+} ions. The ionized silver if binded to proteins causes structural changes in the cell wall and also in the nuclear membranes leading to cell death. Ag^{+} also forms complexes with bases of DNA and RNA inhibiting the micro-organism replication [14]. In addition, metal nanoparticles of silver provide interesting research area owing to the ability of absorption and light emission being biocompatible on nature; then they are suited for nanoparticles optical and biological applications [15].

Silver nanocomposites and their antimicrobial effects have been reported by several researchers. The higher efficiency of silver nanocomposites compared to silver microcomposites of polyamide-AgNPs against *E.coli* was reported in literature [16]. In interesting work [17], researchers showed that Ag^{+} release depends on the nature of the silver antimicrobial and the polymer matrix morphology. The authors concluded that crystallinity and water uptake are very important to silver antimicrobial efficiency.

Recently, it was developed a method chemical reduction for obtain antibacterial silver nanoparticles and inserted them in the LDPE films surface by surface treatment. The antibacterial activity of those films was evaluated by agar diffusion and dynamic shake flask methods, with highly positive results [18]. For instance, the capacity of silver nanoparticles to destroy infectious micro-organisms makes it one of the most powerful antimicrobial agents, an attractive feature against 'super-bugs' resistant to antibiotics [19].

In these sense, the aim of this work is to investigate the effect of insertion of silver nanoparticles in substratum of polypropylene gels and to study their antibacterial activity.

Experimental

Materials

The isotactic Polypropylene (iPP) with MFI = 1.5 dg min^{-1} and Mw = 338,000 g mol^{-1} from Braskem– Brazil was supplied in pellets. Acetylene 99.8 % supplied by White Martins. Silver nanoparticles (AgNPs) were purchased from Sigma Aldrich, reference 576832, lot MKBF5701 V.

Methods

Radiation process

The irradiation process of the pellets placed in nylon bags with acetylene [20, 21] was accomplished in a ^{60}Co gamma source from CBE at dose rate of 5 kGy h^{-1}. The polypropylene irradiation was performed at 12.5 kGy dose monitored by a Harwell Red Perspex 4034 dosimeter. After irradiation, the samples were heated for 1 h at 90 °C to promote the recombination and annihilation of residual radicals.

Melt flow index

The MFI was obtained using a Ceast apparatus in which the samples were flowed through an orifice of 2.0-mm diameter during 10 min under loading of 2.16 kg at 230 °C.

Gel fraction and sol fraction

The gel content was determined by extraction of sample of PP, packed in a stainless steel sieve of 500 mesh, in boiling xylene containing the Irganox 1010 antioxidant for a period of 12 h at 138 °C, ASTM D 2765 [22]. The gel fraction was determined by the relation between the gel mass and the sample multiplied by 100. The initial concentration of the PP for the measure of gel fraction was approximately 0.2 dg cm^{-3}. The sol fraction, soluble part of the sample in beaker was cooled to room temperature to 25 °C when occurred decantation of polypropylene gels. Previous to the deposition, silver nanoparticles were added in the ratios of 0.25; 0.5; 1.0; 2.0; and 4.0 in mass %. After elimination of the xylene it was formed the dried films.

Scanning electron microscopy and energy-dispersive spectroscopy

Scanning electron microscopy was done using an EDAX PHILIPS XL 30. In this work, thin coat of gold was sputter coated onto the samples. It was used also the equipment Tabletop microscope TM-3000, Hitachi for SEM and EDS for additional micrographs.

Transmission electron microscopy

The morphology of the samples was examined by TEM JEOL JEM-2100 operating at an accelerating voltage of

80 kV. The samples were prepared by placing a drop of the gel polypropylene with silver nanoparticles dispersion on a carbon-coated copper grid. The drop was allowed to dry overnight in air. The shape and size of the nanoparticles were characterized by TEM.

Differential scanning calorimetry

Thermal properties of specimens were analyzed using a differential scanning calorimeter DSC 822, Mettler Toledo. The thermal behavior of films was obtained by (1) heating from 25 to 280 °C at a heating rate of 10 °C min^{-1} under nitrogen atmosphere; (2) holding for 5 min at 280 °C; and (3) then cooling to 25 °C and reheating to 280 °C at 10 °C min^{-1}. Melting enthalpy value for 100 % crystalline PP is 209 kJ kg^{-1} [23, 24].

X-ray diffraction

X-ray diffraction (XRD) measurements were carried out in the reflection mode on a Rigaku diffractometer Mini Flex II (Tokyo, Japan) operated at 30 kV voltage and a current of 15 mA with CuKα radiation ($\lambda = 1{,}541841$ Å).

Cytotoxicity tests

The cytotoxicity assay, according to ISO 10993-5:2009 [25], was carried out with the exposure of NCTC L929 cell cultured in a 96 wells microplate to the extract obtained by the immersion of samples in cell culture medium, MEM (minimum Eagle's medium, Sigma Co., São Paulo, Brazil), for 24 h at 37 °C in a CO_2 humidified incubator. After this period, the medium was discarded and replaced with 0.2 mL of serially diluted extract of each sample (50; 25; 12.5; 6.25 %). The cell line was acquired from American Type Culture Collection (ATCC) bank. The cytotoxic effect was evaluated by neutral red uptake (NRU) methodology [26] adapted according to previous work [27]. Negative control used was non-toxic PVC pellets and positive control used was 0.02 % phenol solution. Positive and negative controls were necessary to confirm the performance of the assay. Negative results imply in no cytotoxicity effect on human cells.

Reduction of the colony forming number unit

The antimicrobial activity and efficacy were evaluated according to adaptation of the standard JIS Z 2801: 2010 [28]. Each of the micro-organisms used was activated to the respective stock cultures in appropriate culture medium to obtain inoculate. The cell suspension obtained was tested for each phase standardized in order to obtain a inoculum concentration of 900×10^6 CFU mL^{-1}. The procedure was performed separately for each culture/sample to be tested: 100 mL of inoculum suspension was placed on the specimen, previously sterilized with 70 % alcohol, spreading over an area corresponding to 40×40 mm^2. It was incubated in Petri dishes, for approximately 24 h at 37 °C. After the incubation time, three dilutions were done to facilitate counting of the colonies. Later, another four dilutions were performed, 10×, 100×, 1000×, and 10000×, respectively. Each dilution was carried out using agar Petri plate containing PDA and incubated at 37 °C for 24 h. The percentage reduction in bacterial growth was calculated from the number of surviving bacteria in the Petri dish after incubation for 24 h at 37 °C, multiplied by the dilution.

Results and discussion

Gel fraction/sol fraction and melt flow index

The MFI of PP 12.5 kGy sample decreased to 0.8 ± 0.1 dg min^{-1} in comparison to pristine PP with MFI = 1.5 ± 0.1 dg min^{-1} as indicative of crosslink and/or branching of the material. The value of 3.0 ± 0.1 % for gel fraction of PP 12.5 kGy, follows the reverse, increase with irradiation dose in comparison with pristine PP value 1.0 ± 0.1 %.

Scanning electron microscopy and energy-dispersive spectroscopy

The morphology of the insoluble material retained in the 500 mesh sieve after extraction in boiling xylene is presented in Fig. 1.

The samples deposited on sieve showed spherulites with average diameters of 10–15 μm for gel obtained at PP 12.5 kGy, with predominance of spherical form.

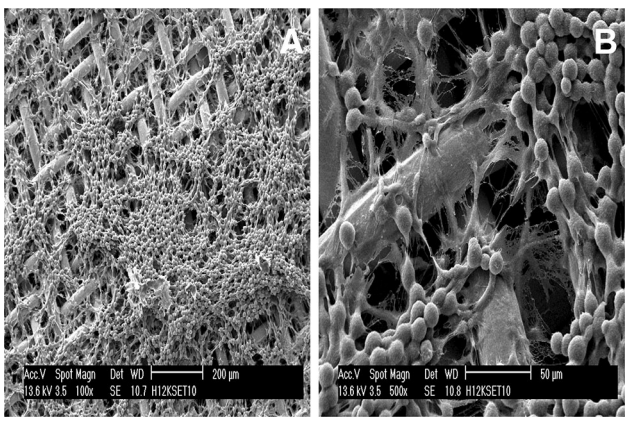

Fig. 1 SEM images of the gel fraction content retained in stainless steel sieve **a** PP 12.5 kGy, 200 μm; **b** PP 12.5 kGy, 50 μm

Figure 2 shows the SEM images and EDX data for gel PP with different percentages of silver nanoparticles. Quantitative analysis of EDX data shows the increase of AgNPs content in the gel, according to the procedure.

Transmission electron microscopy

The TEM image of silver nanoparticles in substratum of polypropylene gels is shown in Fig. 3.

TEM image of the silver nanoparticles from the polypropylene gel matrix illustrates that the spherical shapes of the silver nanoparticles with average size between 40 and 44 nm were distinguished in the surface.

Differential scanning calorimetry

The DSC results are presented in Fig. 4. The curve corresponding to the PP 12.5 kGy gel showed one melting peak,

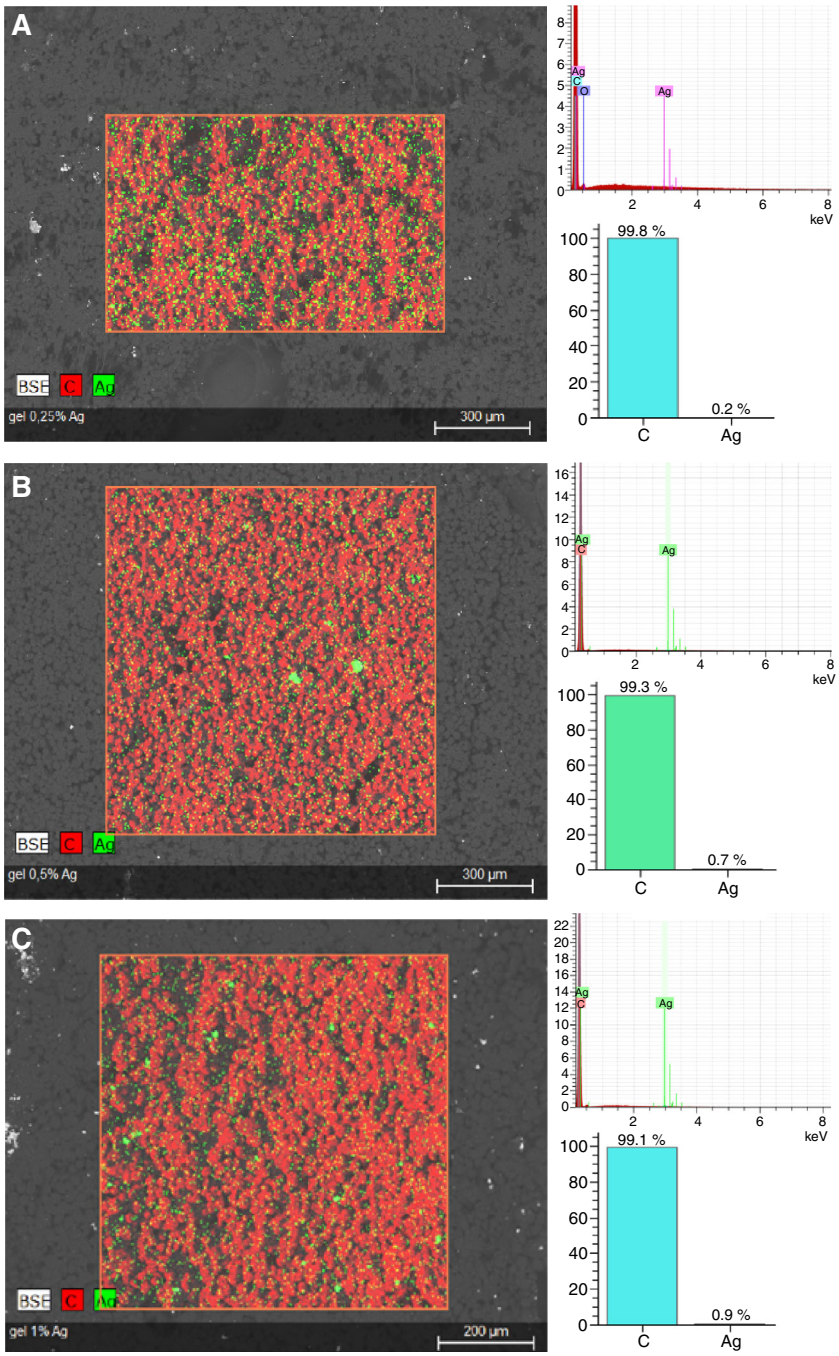

Fig. 2 SEM images and EDS mapping of Ag dispersed in the gel PP modified at 12.5 kGy: **a** 0.25 % AgNPs-GelPP; **b** 0.5 % AgNPs-GelPP; **c** 1 % AgNPs-GelPP; **d** 2 % AgNPs-GelPP; and **e** 4 % AgNPs-GelPP

Fig. 2 continued

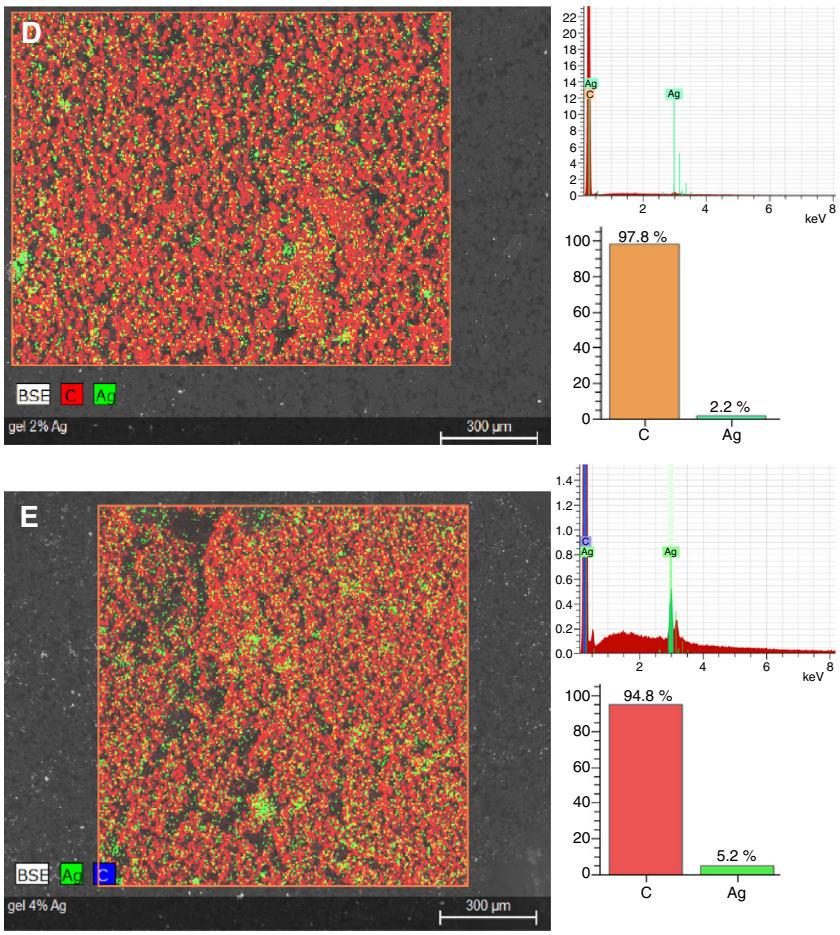

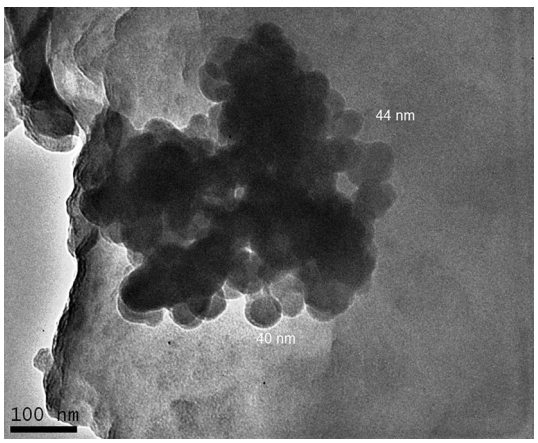

Fig. 3 TEM micrograph of AgNPs-GelPP containing 0.5 mass % silver

whereas two peaks are observed for AgNP-GelPP samples. The gel PP 12.5 kGy peak which appears at 158 °C corresponds to the α-crystal PP form. The two peaks of AgNP-GelPPs melting temperature were observed at 160 and 174 °C, respectively, due to the melting of the β and α-phase similar to the values found in the literature [29]. Silver insertion caused the displacement of α-peak to higher temperature and induced the β-phase formation. The area of this peak increased with Ag concentration until 1 mass % and then decreased for higher concentrations. This behavior confirmed the aggregation of Ag nanoparticles, as seen in Fig. 2d, e. In these cases, 2.0 % AgNPs-GelPP and 4.0 % AgNPs-GelPP, it were reduced their nucleating ability due to the reduction of surface specific area of the nucleant (AgNPs) in function of agglomerates. The same effect has been observed using HNT (halloysite nanotubes) as nucleating agent of PP [30] and wollastonite with PP [31].

The DSC results concerning to the Tm_2 and X_C are presented in Table 1. In Fig. 4, the double melting peaks were observed for AgNPs-GelPP and were attributed to different crystal structures.

Crystallization temperatures T_C (curves not showed) are presented in Table 1. As it can be seen the T_C increases with mass % of AgNPs, behavior also observed in [30].

The crystallinity presented in Table 1 was calculated considering the enthalpy of the α phase. The nucleation of new crystals can be considered, however, as requiring

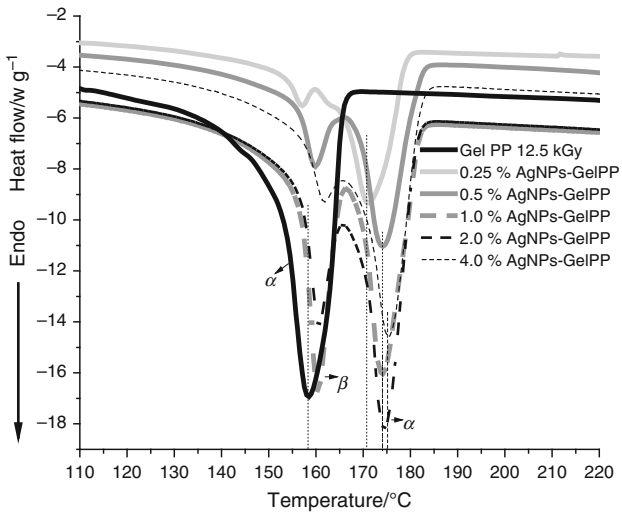

Fig. 4 DSC curves in the melting of the second heating run of AgNPs-GelPP (12.5 kGy) at different silver mass percentages

several mobile molecular segments produced by chain scission and/or the addition of the AgNPs in their close vicinity.

β-crystals were not observed in PP modified by irradiation. In the presence of AgNPs, as shown in Fig. 4, β-phase is observed for AgNPs-GelPP melting curves, suggesting β-nucleation ability, as discussed in the literature [32, 33]. The amount of β-phase in PP depends on the concentration of the additives and cooling conditions during crystallization from the melt [32]. The formation of β-PP under non-isothermal crystallization is also substantiated by XRD experiments. Figure 5 shows the XRD patterns of the AgNPs-GelPP nanocomposite in non-isothermally crystallization.

Gel crystallinity is clearly affected by Ag^+ content, and the lower crystalline phase percentage was verified in Gel 4.0 % AgNPs. According to the literature [17], the susceptibility of the amorphous phase toward water sorption has consequence in the increasing of silver release and in the results of the bactericidal effect.

X-ray diffraction

Fig. 5 shows the X-ray diffraction (XRD) pattern of 1 % AgNPs-GelPP. The peaks observed at $2\theta = 14.2°$; 16.2°; 17.0°; 18.6°; 21.4°; 22.0°; 25.6°; and 28.7°, correspond to the planes (110), (040), (130), (111), (150) + (060), (220), respectively, and were attributed to the α form of PP. For PP and composites exist the β form of PP, plane (300) peak at $2\theta = 16.2°$ [34] and plane (131) + (041) peak at $2\theta = 22°$ that was previously observed [35].

In this result, interplanar distances were obtained from $d_{(110)} = 6.18$ Å, $d_{(300)} = 5.46$ Å, $d_{(04\ 0)} = 5.19$ Å, $d_{(130)} = 4.73$ Å, $d_{(111)} = 4.18$ Å, $d_{(131)\ +\ (041)} = 4.03$ Å, $d_{(150)+(060)} = 3.57$ Å, $d_{(220)} = 3.10$ Å. The X-ray pattern of silver nanoparticles matches the face-centered cubic (fcc) structure of the bulk silver with the broad peaks at 38.4° and 44.5° corresponding to $d_{(111)} = 2.35$ Å and $d_{(200)} = 2.03$ Å, respectively [36–38]. PP modified by irradiation (12.5 kGy) did not show β-crystals nucleating ability [11], while with the addition of AgNPs the β phase occurred.

Cytotoxicity test

In this study, all the tested samples were non-cytotoxic even at 100 % extract concentration. They demonstrated similar behavior to negative control with non-cytotoxicity index ($IC_{50\ \%}$), as shown in Fig. 6.

Cell viability curves were obtained in a graphic traced with cell viabilities percentages against extract concentration. The cytotoxicity index $IC_{50\ \%}$ is obtained in the graphic and means the extract concentration which injures 50 % of the cell population in the assay. The sample with cell viability curve above $IC_{50\ \%}$ line is considered non-cytotoxic and under $IC_{50\ \%}$ line is considered toxic. The cytotoxicity index was obtained by projecting a line from 50 % cellular viability axis to extract concentration. Therefore, the films of AgNPs-GelPP are characterized as non-cytotoxic by cell of mouse and in consequence non-cytotoxic to human cells.

Table 1 DSC data of AgNPs-GelPP during the second run of melting

Samples	Crystallization peak temperature, T_C/°C (± 0.1 %)	Melting peak temperature, T_{m2}/°C (± 0.1 %)		Degree of crystallinity, X_C/% (± 0.5 %)
		T_β	$T\alpha$	
Gel 12.5 kGy	116.5	–	158.2	45.6
Gel 0.25 % AgNPs	130.8	157.0	171.2	50.0
Gel 0.5 % AgNPs	135.9	160.0	174.5	48.4
Gel 1.0 % AgNPs	135.4	160.2	174.1	48.7
Gel 2.0 % AgNPs	136.5	160.6	174.5	48.0
Gel 4.0 % AgNPs	136.5	161.9	175.5	43.5

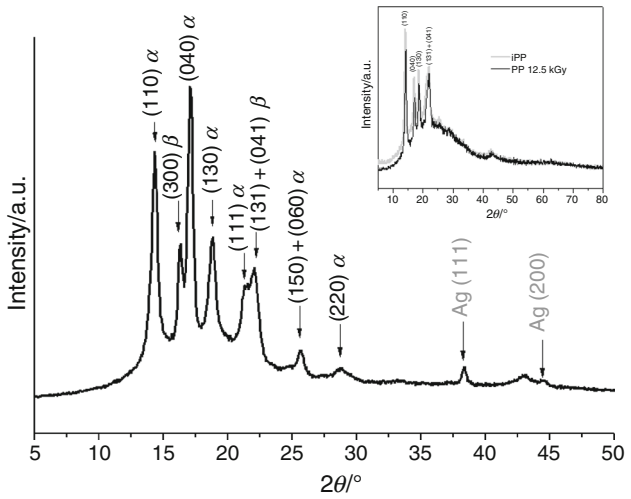

Fig. 5 X-ray diffraction of 1 % AgNPs-GelPP modified 12.5 kGy. Insert is related to previous publication on ref.11

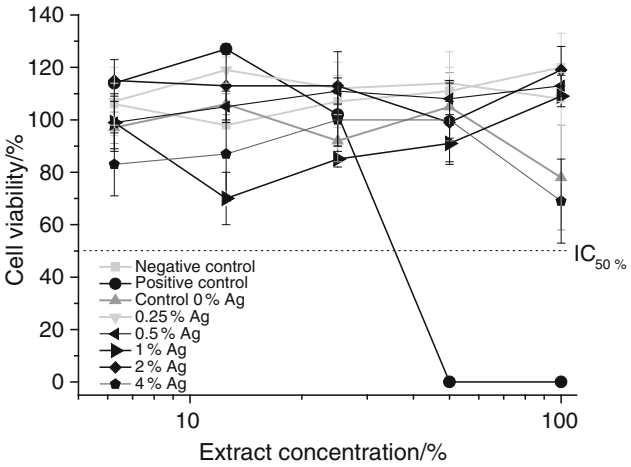

Fig. 6 Cytotoxicity test results of Cell viability curves using neutral red uptake cytotoxicity assay, with NCTC clone 929 cells for different AgNPs-GelPP

Results for reduction of the colony forming number unit

CFU for the films of AgNPs-GelPP, Fig. 7, showed the AgNPs effect for all samples. Relevant effect was observed from 1 % AgNPs, which surviving micro-organisms were 20 % for *E. coli* and 5 % for *S. aureus*. The film with 2 % of AgNPs showed total extermination of *E.coli*, and finally, the proportion of 4 % AgNPs film was 100 % efficient in bactericidal effect for both Gram-negative (*E. coli*) and Gram-positive (*S. aureus*).

The effect is associated to the Ag^{+} release to the cell culture medium in which the water can permeate through the amorphous phase of the polymer performing AgNPs release to the medium. In this sense, differences in crystallinity can corroborate with bacterial effect as previously observed [17].

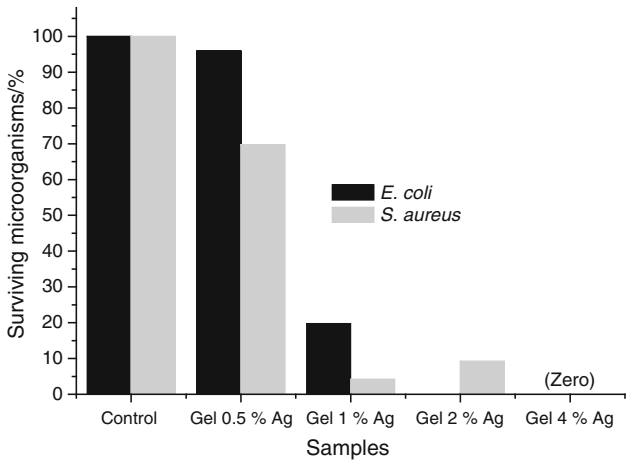

Fig. 7 Surviving micro-organisms after test against *S.aureus* and *E.coli* with different samples AgNPs-GelPP

Conclusions

In conclusion, micro and nanogels promoted by radiation were able to disperse homogeneously AgNPs that in turn induced the β-phase crystallization on polypropylene. The nano-dispersion of Ag improves the antibacterial activity and the gel formed with addition of AgNPs resulted in death of the micro-organism: *S.aureus* and *E.coli* from 1 % AgNPs, and showed non-cytotoxicity for mouse's cell. The lower gel crystallinity was cooperative to higher antimicrobial effect.

Acknowledgements This work was supported by CAPES. The authors acknowledge the Centre of Science and Technology of Materials–CCTM/IPEN, for microscopy analysis (SEM), Project FAPESP 2012-00236-1, Molecular Nanotechnology Group for X-ray diffraction analysis, Project CAPES Pro-equipment's 01/2007, IPEN/CNEN; the technicians Mr. Eleosmar Gasparin and Nelson R. Bueno, for technical support and Companhia Brasileira de Esterilização (CBE) for irradiation of the samples.

References

1. Lugao AB, Otaguro H, Parra DF, Yoshiga A, Lima LFCP, Artel BWH, Liberman S. Review on the production process and uses of controlled rheology polypropylene-gamma radiation versus electron beam processing. Radiat Phys Chem. 2007;76:1688.
2. Lugao AB, Artel BWH, Yoshiga A, Lima LFCP, Parra DF, Bueno JR, Liberman S, Farrah M, Terçariol WR, Otaguro H. Production of high melt strength polypropylene by gamma irradiation. Radiat Phys Chem. 2007;76:1691–5.
3. Spadaro G, Valenza A. Calorimetric analysis of an isotactic polypropylene gamma-irradiated in vacuum. J Therm Anal Calorim. 2000;61:586–96.
4. Chapiro A. Radiation chemistry of polymeric systems. London: Interscience; 1962. p. 385–493.
5. Keene B, Bourham M, Viswanath V, Avci H, Kotek R. Characterization of degradation of polypropylene nonwovens irradiated by γ-ray. J. Appl Polym Sci. 2014;131:1–10.

6. Otaguro H, Lima LFCP, Parra DF, Lugao AB, Chinelatto MA, Canevarolo SV. High-energy radiation forming chain scission and branching in polypropylene. Radiat Phys Chem. 2010;79:318–24.
7. Zagórski ZP. Modification, degradation and stabilization of polymers in view of the classification of radiation spurs. Radiat Phys Chem. 2002;63:9–19.
8. Zagórski ZP, Rafalski A. Free radicals in irradiated unstabilized polypropylene, as seen by diffuse refection absorption-spectrophotometry. Radiat Phys Chem. 1998;52:257.
9. Zagórski ZP. Advances in radiation chemistry of polymers. IAEA-TECDOC-1420. Proceedings of a technical meeting held in Notre Dame, 2003: 21-1.
10. Oliani WL, Parra DF, Riella HG, Lima LFCP, Lugao AB. Polypropylene nanogel: ''Myth or reality''. Radiat Phys Chem. 2012;81:1460–4.
11. Oliani WL, Parra DF, Fermino DM, Riella HG, Lima LFCP, Lugao AB. Study of gel formation by ionizing radiation in polypropylene. Radiat Phys Chem. 2013;84:20–5.
12. Matsuda H, Inoue T, Okabe M, Ukaji T. Study of polyolefin gel in organic solvents. I structure of isotactic polypropylene gel in organic solvents. Polym J. 1987;19:323–9.
13. Dastjerdi R, Montazer MA. A review on the application of inorganic nano-structured materials in the modification of textiles: focus on antimicrobial properties. Colloids Surf B. 2010;79:5–18.
14. Munoz-Bonilla A, Fernández-García M. Polymeric materials with antimicrobial activity. Prog Polym Sci. 2012;37:281–339.
15. Popović ZK, Dragašević M, Krklješ A, Popović S, Jovanović Ž, Tomić S, Stanković VM. On the use of radiation technology for nanoscale engineering of silver/hydrogel based nanocomposites for potential biomedical application. Open Conf Proc J. 2010;1:200–6.
16. Damm C, Münstedt H, Rösch A. The antimicrobial efficacy of polyamide 6/silver-nano-and microcomposites. Mater Chem Phys. 2008;108:61–6.
17. Radheshkumar C, Münstedt H. Antimicrobial polymers from polypropylene/silver composites-Ag + release measured by anode stripping voltammetry. React Funct Polym. 2006;66:780–8.
18. Dehnavi AS, Aroujalian A, Raisi A, Fazel S. Preparation and characterization of polyethylene/silver nanocomposite films with antibacterial activity. J Appl Polym Sci. 2013;127:1180.
19. Sotiriou GA, Pratsinis SE. Engineering nanosilver as an antibacterial, biosensor and bioimaging material. Curr Opin Chem Eng. 2011;1:3.
20. Yoshiga A, Otaguro H, Parra DF, Lima LFCP, Lugao AB. Controlled degradation and crosslinking of polypropylene induced by gamma radiation and acetylene. Polym Bull. 2009;63:397-09.
21. Oliani WL, Parra DF, Lima LFCP, Lugao AB. Morphological characterization of branched PP under stretching. Polym Bull. 2012;68:2121.
22. ASTM D 2765:2006–Standard test methods for determination of gel content and swell ratio of crosslinked ethylene plastics.
23. Mark JE. Physical properties of polymers handbook. 2nd ed. New York: Springer; 2007.
24. Silvestre C, Di-Lorenzo ML, Di-Pace E. Crystallization of Polyolefins. In: Vasile C, editor. Handbook of Polyolefins. 2rd ed. New York: Marcel Dekker; 2000.
25. ISO 10993-5:2009 – Biological evaluation of medical devices. Pat 5: Tests for in vitro cytotoxicity
26. Ciapetti G, Granchi D, Verri E, Savarino L, Cavedagna D, Pizzoferrato A. Application of a neutral red and amido black staining for rapid, reliable cytotoxicity testing of biomaterials. Biomaterials. 1996;17:1259-4.
27. Rogero SO, Malmonge SM, Lugao AB, Ikeda TI, Miyamaru L, Cruz AS. Biocompatibility study of polymeric biomaterials. Artif Organs. 2003;27(5):424–7.
28. JIS Z 2801:2010 - JAPANESE industrial standard - antibacterial products - test for antibacterial activity and efficacy.
29. Zhang B, Chen J, Zhang X, Shen C. Crystal morphology and structure of the β-form of isotactic polypropylene under supercooled extrusion. J Appl Polym Sci. 2011;120:3255-4.
30. Liu M, Guo B, Du M, Chen F, Jia D. Halloysite nanotubes as a novel β-nucleating agent for isotactic polypropylene. Polymer. 2009;50:3022.
31. Ding Q, Zhang Z, Wang C, Jiang J, Li G, Mai K. Non-isothermal crystallization kinetics and morphology of wollastonite-filled β-isotactic polypropylene composites. J Therm Anal Calorim. 2014;115:675–88.
32. Romankiewicz A, Sterzynski T, Brostow W. Structural characterization of α-and β-nucleated isotactic polypropylene. Polym Int. 2004;53:2086–91.
33. Liang GD, Bao SP, Tjong SC. Microstructure and properties of polypropylene composites filled with silver and carbon nanotube nanoparticles prepared by melt-compounding. Mater Sci Eng, B. 2007;142:55-1.
34. Zhang N, Zhang Q, Wang K, Deng H, Fu Q. Combined effect of β-nucleating agent and multi-walled carbon nanotubes on polymorphic composition and morphology of isotactic polypropylene. J Therm Anal Calorim. 2012;107:733–43.
35. Thomas S, Girei AS, La-Juahani AA, Mezghani K, De SK, Atieh MA. Effect of phenol functionalized carbon nanotube on mechanical, dynamics mechanical, and thermal properties of isotactic polypropylene nanocomposites. Polym Eng Sci. 2012;52:525-1.
36. Kim D, Jeong S, Moon J. Synthesis of silver nanoparticles using the polyol process and the influence of precursor injection. Nanotechnology. 2006;17:4019-4.
37. Chudasama B, Vala AK, Andhariya N, Mehta RV, Upadhariya RVJ. Highly bacterial resistant silver nanoparticles: synthesis and antibacterial activities. Nanopart Res. 2010;12:1677-5.
38. Parameshwaran R, Jayavel R, Kalaiselvam S. Study on thermal properties of organic ester phase-change material embedded with silver nanoparticles. J Therm Anal Calorim. 2013;114:845–58.